AIP | Journal of Applied Physics

Electronic structure and magnetic properties of zigzag blue phosphorene nanoribbons

Tao Hu and Jisang Hong

Citation: Journal of Applied Physics **118**, 054301 (2015); doi: 10.1063/1.4927848
View online: http://dx.doi.org/10.1063/1.4927848
View Table of Contents: http://scitation.aip.org/content/aip/journal/jap/118/5?ver=pdfcov
Published by the AIP Publishing

Electronic structure and magnetic properties of zigzag blue phosphorene nanoribbons

Tao Hu and Jisang Hong[a)]
Department of Physics, Pukyong National University, Busan 608-737, South Korea

(Received 22 April 2015; accepted 23 July 2015; published online 3 August 2015)

We investigated the electronic structure and magnetism of zigzag blue phosphorene nanoribbons (ZBPNRs) using first principles density functional theory calculations by changing the widths of ZBPNRs from 1.5 to 5 nm. In addition, the effect of H and O passivation was explored as well. The ZBPNRs displayed intra-edge antiferromagnetic ground state with a semiconducting band gap of ~0.35 eV; and this was insensitive to the edge structure relaxation effect. However, the edge magnetism of ZBPNRs disappeared with H-passivation. Moreover, the band gap of H-passivated ZBPNRs was greatly enhanced because the calculated band gap was ~1.77 eV, and this was almost the same as that of two-dimensional blue phosphorene layer. For O-passivated ZBPNRs, we also found an intra-edge antiferromagnetic state. Besides, both unpassivated and O-passivated ZBPNRs preserved almost the same band gap. We predict that the electronic band structure and magnetic properties can be controlled by means of passivation. Moreover, the edge magnetism can be also modulated by the strain. Nonetheless, the intrinsic physical properties are size independent. This feature can be an advantage for device applications because it may not be necessary to precisely control the width of the nanoribbon. © *2015 AIP Publishing LLC*. [http://dx.doi.org/10.1063/1.4927848]

I. INTRODUCTION

Two-dimensional (2D) materials display many intriguing physical properties, not found in bulk structure because the electronic structure is substantially altered from its three-dimensional characteristics. Recently, a newly found 2D material so called black phosphorus has drawn considerable attention due to the successful exfoliation of few-layer black phosphorus (phosphorene),[1–4] and it has displayed remarkable physical properties. Unlike the graphene, this 2D black phosphorene monolayer has a direct band gap of 1.0 eV.[2] Besides, few layers black phosphorene based field effect transistors have high mobility and high on/off ratio. Furthermore, anisotropic electrical[1] and optical properties[5] have been found. Due to these peculiar physical properties, the phosphorene is considered as a potential candidate for next-generation 2D material for diverse device applications.[2,5–9] One can find several theoretical and experimental studies on the black phosphorus layer,[10–19] nanotube, and nanoribbons.[6,20,21] These studies reveal that the band gap strongly depends on the geometry because the zigzag nanoribbons show metallic band structure while armchair nanoribbons are semiconductors, whereas the nanotube structures show chiral dependent band structures. Thus, the electronic band structure is significantly modified by the structure.

Since the phosphorene consists of non-magnetic (NM) phosphorus atom, this 2D materials has no spin polarized state. Indeed, the same argument can be applied to the graphene because the carbon atom is also a non-magnetic element. However, the edge magnetism has been reported in graphene nanoribbons.[22,23] Motivated by this, the edge magnetism was explored in the black phosphorene nanoribbons. Interestingly, the magnetic state appeared at the edge atoms in an ideal nanoribbon structure, but the edge magnetism vanished after the structure relaxation.[24,25] Thus, all the black phosphorene nanoribbons do not show spin polarized state. As compared with the black phosphorene, the blue phosphorene[26] has a different characteristic in the structural point of view. The black phosphorene has an orthorhombic primitive cell while the blue phosphorene possesses a hexagonal one. This structural disparity will definitely result in different band structure and magnetic property. In addition, hexagonally bonded zigzag nanoribbons consisted solely by boron, nitrogen, and carbon have been found to show edge ferromagnetic (FM) ordering.[27] The edge magnetism is claimed to be generic in zigzag-edge terminated honeycomb nanostructures.[28] The blue phosphorene can satisfy these conditions. Thus, in this report, we will explore the potential edge magnetism in the blue phosphorene zigzag nanoribbons (BPZNRs) by changing the width. In particular, the edge magnetism will bring an interesting issue in the study of nanoribbons solely consisted of 2*p* elements. Previous studies show that the edges passivation with various species present different properties,[21] and also an external strain on the nanoribbons can change the edges magnetism drastically.[29] Therefore, we will explore the effect of edge passivation and strain effect on the edge magnetism as well.

II. NUMERICAL METHOD

We have performed spin polarized first-principles calculation based on density functional theory with the generalized gradient approximation (GGA) of Perdew-Burke-Ernzerhof.[30] The Vienna *ab-initio* Simulation Package (VASP)[31–34] is used. A plane-wave basis set with an energy cutoff of 500 eV is employed. All calculations are chosen to

a)Author to whom correspondence should be addressed. Electronic mail: hongj@pknu.ac.kr.

converge the total energy to 0.01 eV, and the energy convergence criterion was set to 10^{-5} eV. A two-dimensional blue phosphorene layer has two P atoms arranged in a hexagonal primitive unit cell, and the lattice constant of the primitive unit cell is 3.30×3.30 Å. We used a vacuum distance of 20 Å in the z direction and at least 15 Å in the x direction to avoid an artificial interaction from neighboring unit cell. Entire calculations have been performed with a $(1 \times 41 \times 1)$ k-mesh scheme.

III. RESULTS AND DISCUSSIONS

In Fig. 1(a), we showed the schematic illustration of zigzag blue phosphorene nanoribbon (ZBPNR) considered in our calculations. The ribbon was obtained by cutting the blue phosphorene layer along the y direction. We defined the width (in the x direction) of the nanoribbons by NL referring to the number of P dimer lines. To investigate the width dependent physical properties, we explored four types of nanoribbons ($N =$ 10, 13, and 18). Then, the corresponding width of each nanoribbon is 1.5, 2.6, 3.7, and 5.0 nm, respectively. Indeed, the edge magnetism of black phosphorene nanoribbon was strongly affected by the edge relaxation effect.[24] For instance, the pristine black phosphorene layer with an ideal structure had magnetic moments at the edge atoms, but the magnetic states vanished after structure relaxation. Thus, we first examined the edge magnetism of ZBPNRs affected by the structure relaxation. Unlike the black phosphorene nanoribbons, we observed that both unrelaxed and relaxed ZBPNRs displayed the same magnetic behavior. We then explored the magnetic ground state of each ribbon by performing the total energy calculation in NM state, FM, and anti-ferromagnetic (AFM). For AFM states, three different magnetic configurations were investigated as indicated in Fig. 1(b). All these magnetic configurations were initially assigned a magnetic moment based on magnetic ordering shown in Fig. 1(b) and then we performed structure relaxation. Fig. 2(a) showed the calculated results of the total energy differences among the NM, FM, and AFM states. First of all, the total energy difference between NM and FM states revealed that the FM state was much more stable than NM state. Besides, we found the similar behavior in the total energy difference between NM and AFM-1 states. This result implies that the FM and AFM-1 states are nearly degenerated. We also observed that the AFM-2 and AFM-3 states were degenerated. Finally, the AFM-2 or AFM-3 state had approximately ~60 meV lower energy than FM or AFM-1 state. Consequently, the ZBPNRs had an intra-edge antiferromagnetic coupling in the ground state. Furthermore, a 60 meV of exchange energy in the magnetic systems is larger than the room-temperature thermal energy (K_BT). This may indicate that the AFM-2 or AFM-3 state will be stable at room-temperature. Fig. 2(b) showed the spin densities of ZBPNRs in AFM-2 and AFM-3 states. Here, we only presented the result of ZBPNR with 10L width (2.7 nm in width) because all other systems displayed the similar trend. We set a relatively low isosurface value 0.002 e/Å^3 for the spin density plot. Only four edge atoms were spin polarized while all the other P atoms showed non-spin polarized states. A magnetic moment of 0.2 μ_B per edge atom was found on the four edge atoms. The other three ZBPNRs with different width had the same results. We displayed the density of states (DOS) for one of the edge atoms in Fig. 2(c). The DOS showed that the magnetic moment at the edge atom mostly originated from p_z orbital perpendicular to the nanoribbons plane, and this agreed with the spin density plot in Fig. 2(b). In Fig. 2(d), we showed the calculated band structure of 10L-ZBPNR in the ground state, and the calculated band gap was 0.35 eV. Note that the two-dimensional blue phosphorene layer has a band gap of 1.86 eV. Thus, the band gap was greatly suppressed in nanoribbon geometry. This suppression of band gap originates from the edge states observed near the Fermi level. For other systems, we found the similar band structures.

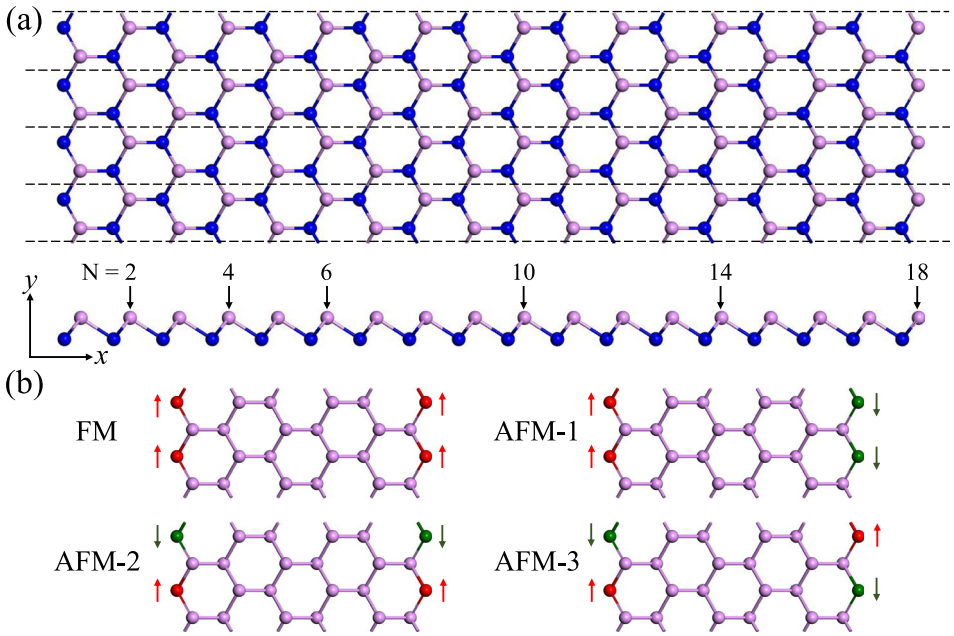

FIG. 1. (a) Schematic top and side views of ZBPNRs. The unit cells are periodically expanded in the y direction. The numbers of P dimer lines along the x direction indicate the width of ZBPNRs. (b) Illustration of the magnetic ordering of the four different magnetic states: FM, AFM-1, AFM-2, and AFM-3.

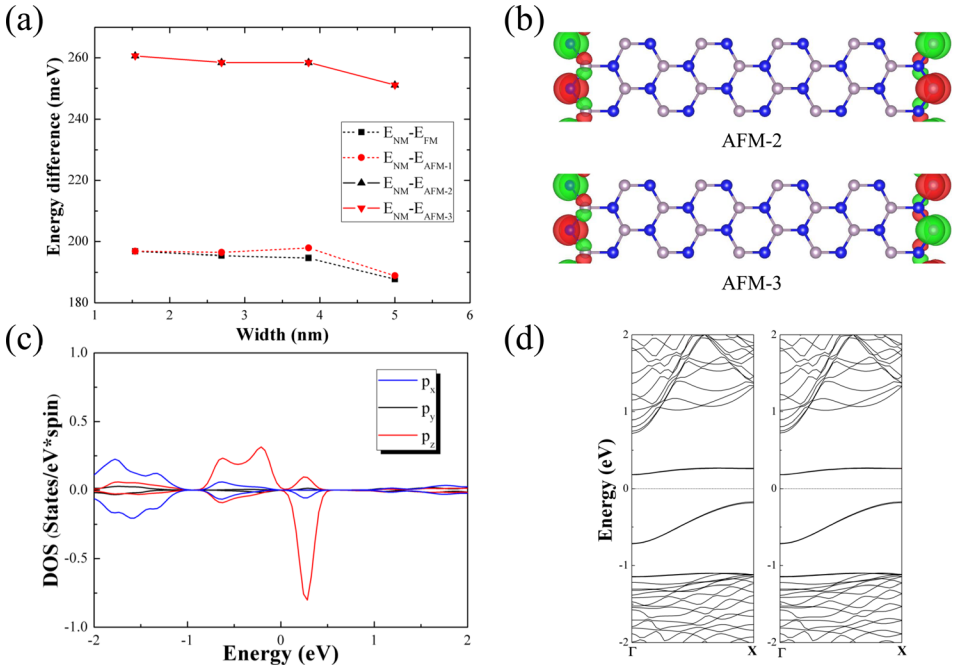

FIG. 2. (a) Total energy difference of the four magnetic states with respect to the NM state as a function of the width of nanoribbons. (b) Spin densities of 10L-ZBPNRs in AFM-2 and AFM-3 states; the isosurface value is set to be 0.002 e/Å^3. The red and blue spheres represent the positive and negative, respectively. (c) Projected DOS of one of P atom at the edge. (d) Calculated band structures of 10L-ZBPNRs in AFM-2 and AFM-3 states.

To further investigate the edge effects in the electronic band structure and magnetic property of ZBPNRs, we explored the ZBPNRs with edges passivated by H and O atoms. In the case of H-passivation, the magnetism totally disappeared, and the ZBPNRs showed non-magnetic state. This same feature was found in the studies of graphene nanoribbons and black phosphorene nanoribbons. Despite this non-magnetic behavior, we found a very interesting band structure in the H-passivated ZBPNRs. As displayed in Fig. 3, the band gap of H-passivated system was greatly enhanced as compared with the unpassivated system. The calculated band gap was about 1.77 eV, and this is very close to that of 2D blue phosphorene layer. In Fig. 2(d) for the band structure of unpassivated 10L-ZBPNR, we observed low-lying bands originated from the edge atoms. However, this band disappeared after the H-passivation, and the band splitting between conduction band minimum and valence band maximum was enhanced. From the Bader charge analysis,[35] the electron charge transfer of 0.5 e from a phosphorus atom to one H atom was obtained. The two H atoms at the edge had a spin singlet state, and this resulted in zero magnetic moment. Due to this anti-symmetric spin configuration, the electrons tended to accumulate in the center two H atoms, and this caused the enhanced Coulomb repulsive interaction. Therefore, the band gap was greatly enhanced in the H-passivated system.

For O-passivation ZBPNRs, we performed the same process to search the ground state spin configuration. Fig. 4(a) showed the total energy differences. In general, the NM state was more stable than the FM and AFM-1 states although the FM state of 6L-ZBPNR was 1–2 meV more stable than the NM state. However, we found that the AFM-2 or AFM-3 state

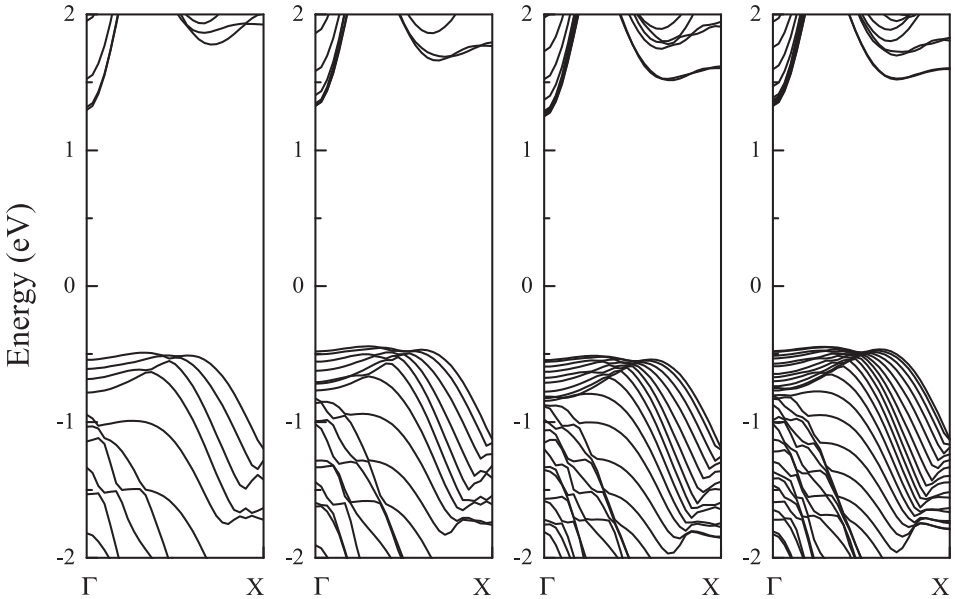

FIG. 3. Calculated band structures of the H-passivated ZBPNRs with different width.

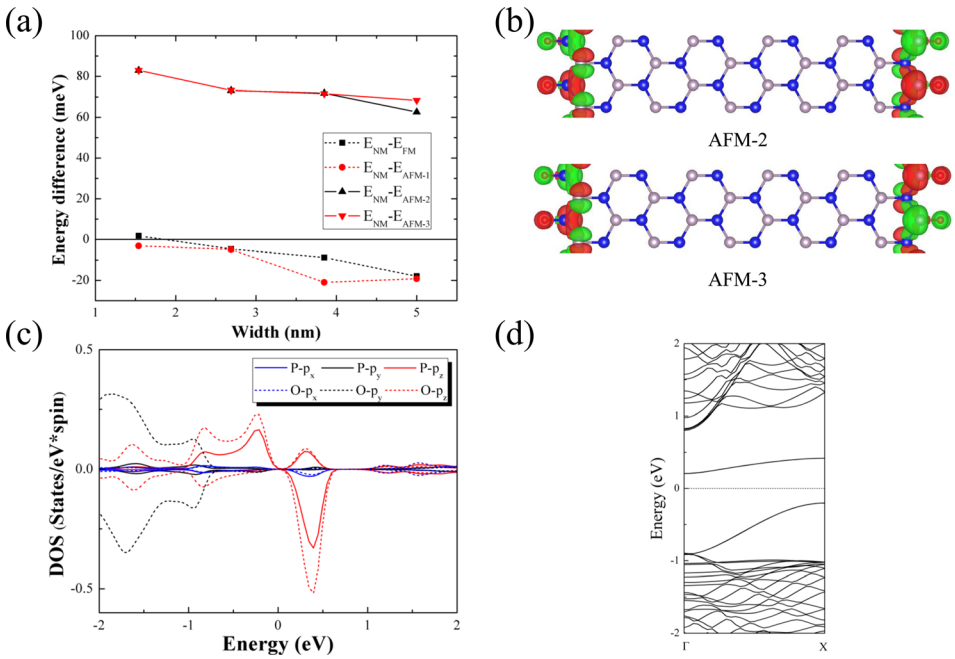

FIG. 4. (a) Total energies difference of the four magnetic states of O-passivated ZBPNRs with respect to the NM state as a function of the width of nanoribbons. (b) Spin densities of O-passivated 10L-ZBPNRs in AFM-2 and AFM-3 states, the isosurface value is set to be 0.002 e/Å^3. The red and blue spheres represent the positive and negative, respectively. (c) Projected DOS of one of P and O atoms at the edge. (d) Calculated band structure of O-10L-ZBPNRs in AFM-2, AFM-3 state possesses the same band structure.

was more stable than the NM state. Besides, similar to the unpassivated ZBPNRs, the total energy difference between AFM-2 and AFM-3 states was also close to each other so that both states were nearly degenerated. As a result, we found an intra-edge AFM ground state, and this state was the same as that of unpassivated ZBPNRs. Fig. 4(b) showed the spin densities of O-passivated 10L-ZBPNR in the AFM-2 and AFM-3. In the O-passivated system, we observed magnetic moment in both edge O and P atoms. The calculated magnetic moment in P atom was 0.10 μ_B, and the O atom maintained a magnetic moment of 0.16 μ_B. Fig. 4(c) shows the DOS on the edge O and P atoms. It was found that the p_z orbital of O and P atoms mainly contributed to the edge magnetism. From the band structure shown in Fig. 4(d), we observed that the band gap of O-passivated ZBPNR was 0.41 eV. Thus, we find that the O-passivation does not strongly disturb the electronic band structure and magnetic properties of the ZBPNRs. All these results imply that the band structure and edge magnetic state of ZBPNRs are strongly dependent on the type of passivation element. Nonetheless, the electronic and magnetic properties of the ZBPNRs show a very weak dependence on their width. This implies that it may not be necessary to precisely control the width of the nanoribbon to produce the ZBPNRs with uniform electronic and magnetic properties. This property will be a great advantage for nanoscale electronic device applications.

To explore the effect of strain on the magnetism, both compressive and tensile strains up to 10% were applied along the periodic direction of the 10L-ZBPNR. First of all, we found that both FM and AFM-1 had the same total energy. Similarly, both AFM-2 and AFM-3 had the same total energy. This implies that the edge-to-edge interaction is negligible even in the presence of external strain. We thus focus on the intra-edge magnetic interaction. As shown in Fig. 5, we found that the strain could change the magnetic ground state of ZBPNR. In particular, the magnetic ground state was strongly affected by the compressive strain. For instance, the change in the magnetic ground state from AFM-2 to FM was observed

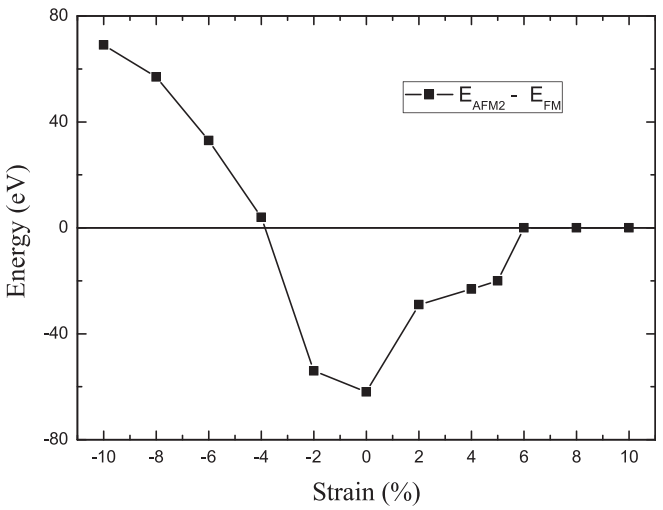

FIG. 5. Calculated energy differences between AFM-2 state and FM state under external strain. The negative percentage means compressive strain, and the tensile strain is positive.

at 4% of the compressive strain. On the other hand, we found that the edge magnetic state vanished at 6% of tensile stain. Indeed, the similar behavior was observed in black phosphorene nanoribbon.[29] Along with the change in the magnetic state, the band structure was also modified due to the external strain. We found that the band gap disappeared at the compressive strain (>4%) and the ZBPNR became metallic. For a tensile strain larger than 6%, we also observed a transition from semiconductor to metal.

IV. CONCLUSION

In summary, we investigated the electronic structure and edge magnetism of zigzag blue phosphorene nanoribbons by changing the width. Here, four different widths of 1.5, 2.7, 3.8, and 5.0 nm were considered. In addition, we explored the effect of H and O passivation at the edge. We found an

intra-edge antiferromagnetic ground state in unpassivated ZBPNRs, and the edge magnetism of ZBPNRs was insensitive to the structure relaxation. The magnetic moment was localized on the edge P atoms, and the spin polarization originated from p_z orbital. In addition, we found that the ZBPNRs had semiconducting band gaps. After H passivation, the edge magnetism disappeared, and also the band gap was greatly enhanced. The calculated band gap was ~1.77 eV in 10L-ZBPNRs. It should be noted that this value of band gap is almost the same as that of two-dimensional blue phosphorene layer. However, the edge magnetism reappeared in the O-passivated ZBPNRs. The O-passivated ZBPNRs showed the same magnetic ground state like in the unpassivated system. In addition, the band gap of O-passivated system was not strongly modified from that of the unpassivated nanoribbon. We found that the edge magnetism was influenced significantly by the strain effect. A compressive strain of larger than 4% tunes AFM ground state to FM along the same edge, while the tensile strain makes the edge magnetism vanish at 6%. The semiconductor-metal transition was also observed due to an external strain effect. Overall, we propose that the electronic band structure and magnetic properties can be manipulated by means of passivation and strain. However, the fundamental physical properties are less sensitive to the size of the ribbon, and this characteristic can be an advantage for device applications.

ACKNOWLEDGMENTS

This research was supported by Basic Science Research Program through the National Research Foundation of Korea (NRF) funded by the Ministry of Education, Science and Technology (Grant No. 2013R1A1A2006071) and by the Supercomputing Center/Korea Institute of Science and Technology Information with supercomputing resources including technical support (KSC-2015-C3-021).

[1]L. Li, Y. Yu, G. J. Ye, Q. Ge, X. Ou, H. Wu, D. Feng, X. H. Chen, and Y. Zhang, Nat. Nanotechnol. **9**, 372 (2014).
[2]H. Liu, A. T. Neal, Z. Zhu, Z. Luo, X. Xu, D. Tománek, and P. D. Ye, ACS Nano **8**, 4033 (2014).
[3]W. Lu, H. Nan, J. Hong, Y. Chen, C. Zhu, Z. Liang, X. Ma, Z. Ni, C. Jin, and Z. Zhang, Nano Res. **7**, 853 (2014).
[4]A. Castellanos-Gomez, L. Vicarelli, E. Prada, J. O. Island, K. L. Narasimha-Acharya, S. I. Blanter, D. J. Groenendijk, M. Buscema, G. A. Steele, J. V. Alvarez, H. W. Zandbergen, J. J. Palacios, and H. S. J. van der Zant, 2D Mater. **1**, 025001 (2014).
[5]J. Qiao, X. Kong, Z.-X. Hu, F. Yang, and W. Ji, Nat. Commun. **5**, 4475 (2014).
[6]V. Tran and L. Yang, Phys. Rev. B **89**, 245407 (2014).
[7]S. Zhang, J. Yang, R. Xu, F. Wang, W. Li, M. Ghufran, Y.-W. Zhang, Z. Yu, G. Zhang, Q. Qin, and Y. Lu, ACS Nano **8**, 9590 (2014).
[8]F. Xia, H. Wang, and Y. Jia, Nat. Commun. **5**, 4458 (2014).
[9]S. Das, M. Demarteau, and A. Roelofs, ACS Nano **8**, 11730 (2014).
[10]A. S. Rodin, A. Carvalho, and A. H. Castro Neto, Phys. Rev. Lett. **112**, 176801 (2014).
[11]S. P. Koenig, R. A. Doganov, H. Schmidt, A. H. C. Neto, and B. Özyilmaz, Appl. Phys. Lett. **104**, 103106 (2014).
[12]R. Fei and L. Yang, Nano Lett. **14**, 2884 (2014).
[13]V. Tran, R. Soklaski, Y. Liang, and L. Yang, Phys. Rev. B **89**, 235319 (2014).
[14]A. N. Rudenko and M. I. Katsnelson, Phys. Rev. B **89**, 201408 (2014).
[15]M. Buscema, D. J. Groenendijk, S. I. Blanter, G. A. Steele, H. S. J. van der Zant, and A. Castellanos-Gomez, Nano Lett. **14**, 3347 (2014).
[16]I. Khan and J. Hong, New J. Phys. **17**, 023056 (2015).
[17]J. Dai and X. C. Zeng, J. Phys. Chem. Lett. **5**, 1289 (2014).
[18]T. Hu and J. Hong, J. Phys. Chem. C **119**, 8199 (2015).
[19]A. Hashmi and J. Hong, J. Phys. Chem. C **119**, 1859 (2015).
[20]H. Guo, N. Lu, J. Dai, X. Wu, and X. C. Zeng, J. Phys. Chem. C **118**, 14051 (2014).
[21]X. Peng, A. Copple, and Q. Wei, J. Appl. Phys. **116**, 144301 (2014).
[22]M. Fujita, K. Wakabayashi, K. Nakada, and K. Kusakabe, J. Phys. Soc. Jpn. **65**, 1920 (1996).
[23]H. Lee, Y.-W. Son, N. Park, S. Han, and J. Yu, Phys. Rev. B **72**, 174431 (2005).
[24]Z. Zhu, C. Li, W. Yu, D. Chang, Q. Sun, and Y. Jia, Appl. Phys. Lett. **105**, 113105 (2014).
[25]M. U. Farooq, A. Hashmi, and J. Hong, ACS Appl. Mater. Interfaces **7**, 14423 (2015).
[26]Z. Zhu and D. Tománek, Phys. Rev. Lett. **112**, 176802 (2014).
[27]S. Okada and A. Oshiyama, Phys. Rev. Lett. **87**, 146803 (2001).
[28]S. Bhowmick, A. Medhi, and V. B. Shenoy, Phys. Rev. B **87**, 085412 (2013).
[29]Y. Du, H. Liu, B. Xu, L. Sheng, J. Yin, C.-G. Duan, and X. Wan, Sci. Rep. **5**, 8921 (2015).
[30]J. P. Perdew, K. Burke, and M. Ernzerhof, Phys. Rev. Lett. **77**, 3865 (1996).
[31]G. Kresse and J. Hafner, Phys. Rev. B **47**, 558 (1993).
[32]G. Kresse and J. Hafner, Phys. Rev. B **49**, 14251 (1994).
[33]G. Kresse and J. Furthmüller, Comput. Mater. Sci. **6**, 15 (1996).
[34]G. Kresse and J. Furthmüller, Phys. Rev. B **54**, 11169 (1996).
[35]W. Tang, E. Sanville, and G. Henkelman, J. Phys. Condens. Matter **21**, 084204 (2009).